HELICOIDAL ANTIPHASE SPIN ORDERING IN HEXAGONAL FERRITES OF THE $BaSc_xFe_{12-x}O_{19}$ *(M) SYSTEM*

O. P. ALESHKO-OZHEVSKIĬ, R. A. SIZOV, I. I. YAMZIN, and V. A. LUBIMTSEV

Submitted April 11, 1968

Zh. Eksp. Teor. Fiz. 55, 820–830 (September, 1968)

The $BaSc_xFe_{12-x}O_{19}$(M) system was studied by the neutron-diffraction technique at 293 and 77°K in fields up to 5 kOe applied perpendicularly to the scattering vector. The magnetic superstructure in the neutron-diffraction patterns at 77°K was explained assuming that an antiphase conical helix was formed by the total magnetic moments of certain blocks of the crystal unit cell. Collinear ordering of the spins of the magnetic ions was assumed to exist within these blocks.

1. ATOMIC STRUCTURE AND MAGNETIC PROPERTIES OF M-TYPE FERRITES

THE atomic structure of hexagonal ferrites is simplest in the M-type compounds with the chemical formula $Me^{2+}Me^{3+}_{12}O_{19}$, where Me^{2+} is a large cation, for example Ba^{2+}, and Me^{3+} is a cation of moderate size (Fe^{3+}, Al^{3+}, etc.). Among the M-type ferrites the simplest is $BaFe_{12}O_{19}$, which is the analog of the naturally occurring mineral magnetoplumbite.

X-ray diffraction investigations[1,2] have established the space groups and the coordinates of atoms in hexagonal ferrites, including ferrites of the M type. Figure 1 shows a section through the unit cell of the ferrite $BaFe_{12}O_{19}$, taken from [2]. Bearing in mind the nature of the packing of oxygen layers, perpendicular to the hexagonal C axis, and the distribution of iron ions in octahedral and tetrahedral positions, we can regard the structure of this ferrite as an assembly of four-layer spinel (cubic) blocks joined by hexagonal oxygen layers which bind these blocks. This binding function is performed by an oxygen layer in which each of the four O^{2-} ions is replaced by a Ba^{2+} ion. On the other hand, if we begin with a binding layer, we see that this layer and the layers immediately below and above it form a sequence of three hexagonally packed layers. These hexagonal blocks are bound by a two-layer spinel block. We call it the spinel block because the nature of the cation distribution in it is the same as in the spinel structure. The nonuniformity of the ordering of oxygen layers along the C axis produces geometrically different tetrahedra and octahedra in the structure. Moreover, there are sites with a fivefold coordination in the layers containing barium atoms. Thus, we may expect that the nature of the distribution of various cations in hexagonal ferrites can assume a greater variety of form than in cubic ferrites.

Earlier investigations of the magnetic properties of various analogs of magnetoplumbite have demonstrated that all of them are uniaxial magnetic materials with an easy magnetization axis, parallel to the C axis, and with a strong magnetic anisotropy.[3-5] Gorter[5] compared the values of the magnetization in barium ferrites and possible variants of the ordering of the Fe^{3+} moments using the indirect exchange theory of Kramers and Anderson[6,7] and found that these compounds can be described by an axial model of spin ordering with the spins parallel to the C axis. The ordering of the spin magnetic moments suggested by Gorter is shown in Fig. 1. Gorter's scheme has been confirmed experimentally by a neutron-diffraction investigation of $BaFe_{12}O_{19}$ crystals.[8] The same spin ordering obviously applies also to the (Ba, Sr, Pb, Ca)$Me^{3+}_{12}O_{19}$ structures in which all the Me^{3+} are magnetically active and equivalent. However, when some of the Fe^{3+} ions are replaced by nonmagnetic ions, a selective distribution of the latter may produce nonmagnetic layers and the collinear magnetic structure may not be obtained. Departures from the axial ordering have been reported in several papers[9,11] for the M-type ferrites in which some Fe^{3+} ions have been replaced by $Ti^{4+} + Co^{2+}$ or $Ir^{4+} + Zn^{2+}$ pairs.

Perekalina and Cheparin[12] recently reported some anomalies in the magnetic properties of the $BaSc_xFe_{12-x}O_{19}$(M) system. They discovered a complex behavior of the magnetic anisotropy, which has an easy magnetization plane or axis, depending on the composition and temperature. The temperature dependence of the magnetization of ferrites belonging to this system is particularly interesting. When the concentration of scandium is increased, the saturation value of the moment decreases considerably. Moreover, in compositions with a high concentration of scandium ($x \geq 1.2$), a decrease of the magnetization is observed when the

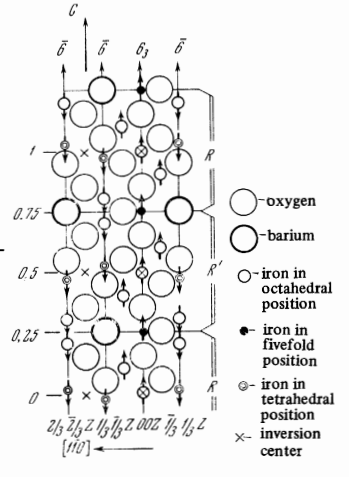

FIG. 1. Atomic structure and spin directions of magnetic ions in the unit cell of $BaFe_{12}O_{19}$ according to [2,5].

temperature is lowered below a certain value. Perekalina and Cheparin suggested that this effect can be explained by the different temperature dependences of the magnetization of the different sublattices.

2. EXPERIMENTAL STUDIES AND NEUTRON-DIFFRACTION INVESTIGATION

The investigation reported in the present paper was carried out using single crystals of the $BaSc_xFe_{12-x}O_{19}$ system with the following values of x: 0, 0.5, 1.2, 1.4, and 1.8. These single crystals were prepared by the spontaneous crystallization method from a molten solution. The crystals were prismatic and measured $1 \times 2 \times 4$ mm. Table I gives Perekalina and Cheparin's values[12] of the unit cell parameters c and a, which vary in a regular manner with the concentration of scandium.

We used these samples to obtain neutron-diffraction patterns at temperatures of 77 and 293°K, as well as above the Curie point. We also investigated the dependence of the reflection intensities on a magnetic field up to 5000 Oe, applied at right-angles to the scattering vector ε. We used a beam of unpolarized neutrons having a wavelength of 1.05 Å. We obtained the following results.

A. $BaFe_{12}O_{19}$ ferrite. We compared the measured reflection intensities I_{exp} with their theoretical values I_{theor}. We calculated the theoretical values using the atomic coordinates found in [1, 2]. Comparison of the measured and calculated intensities was carried out for ten basal reflections $00l$ and eight "nonbasal" reflections $h0l$ and $hk0$.

The basal reflections $00l$, which were practically free of the magnetic contribution, showed good agreement between I_{exp} and I_{theor}, with the R factor of ~6%. The value of the R factor for the nonbasal reflections was ~12%, which was probably due to errors in the determination of the nuclear contribution to the intensity I^n_{exp} in the case of mixed reflections at temperatures above the Curie point. The experimental values of the magnetic contributions agreed well with the uniaxial magnetic structure model proposed by Gorter for ferrites of this type.[5] The value of the R factor for the magnetic reflections was, according to our results, ~15%. Thus, we could assume that the magnetic structure of the ferrite $BaFe_{12}O_{19}$ at 293°K was in agreement with the model shown in Fig. 1.

Next, we compared the intensities of the basal reflections for all the compositions by reducing them to the absolute scale using the value of the nuclear contribution to the intensity of the 006 reflection. To calculate the primary extinction coefficient E_p, we used the value of the mosaic block thickness $t = 10^{-3}$ cm.[13] To determine the angular distribution (scatter) parameter η of the mosaic blocks, we used ten nuclear $00l$ reflections of $BaFe_{12}O_{19}$. The value of η was ~15″ at 293°K and 20″ at 77°K. These values of t and η were used to calculate the reflection intensities for other compositions. The magnetic structure factors were calculated using the form factor for Fe^{3+} taken from [14].

B. $BaSc_{1.8}Fe_{10.2}O_{19}$ ferrite. This compound had the highest concentration of scandium among the investigated samples. Figure 2 shows the neutron-diffraction patterns of the basal planes of a single crystal of this compound at room and liquid nitrogen temperatures. The neutron-diffraction pattern at 293°K (Fig. 2a) included a series of structure reflections of the $00l$ type, which contained some magnetic contribution. To select the possible models which could explain the neutron-diffraction patterns, we used the results of magnetic investigations.

An easy magnetization plane was exhibited by this compound in the temperature range 125–355°K. Figure 3 shows possible spin ordering models which have an easy magnetization plane. The model shown in Fig. 3a does not agree with the neutron-diffraction data because in this case the neutron-diffraction patterns of the basal reflections should have the antiferromagnetic components (σ_a) of the spin moments (σ) of the structure blocks R and R′. In this case, we can expect reflections of purely magnetic origin at points forbidden for the nuclear reflections; their indices are $00l$, where l is an odd integer. Since this is not observed, we have assumed the model shown in Fig. 3b in which the spin axes of the R and R′ blocks of the unit cell (Fig. 1) are

Table I. Unit cell parameters of crystals of the $BaSc_xFe_{12-x}O_{19}$(M) system[12]

Ferrite	c, Å	a, Å
$BaFe_{12}O_{19}$	23.18	5.78
$BaSc_{0.5}Fe_{11.5}O_{19}$	23.30	5.90
$BaSc_{1.2}Fe_{10.8}O_{19}$	23.49	5.90
$BaSc_{1.4}Fe_{10.6}O_{19}$	23.53	5.93
$BaSc_{1.8}Fe_{10.2}O_{19}$	23.61	5.96

The error in the determination of c was ±0.004 Å and that in the determination of a was ±0.002 Å.

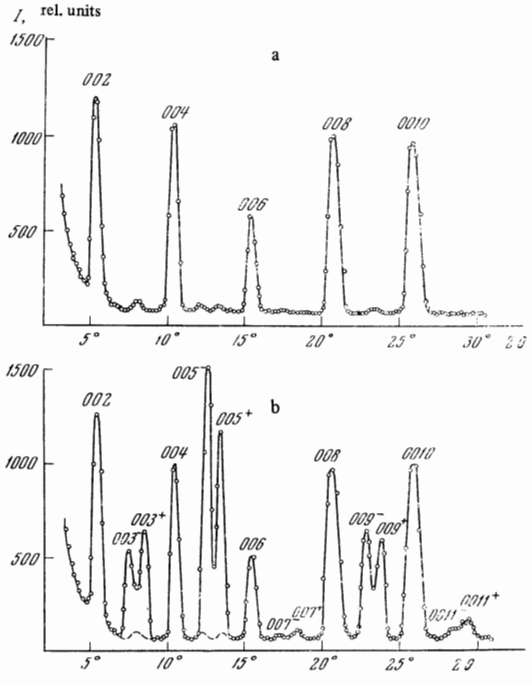

FIG. 2. Neutron-diffraction patterns of a family of the basal planes of a $BaSc_{1.8}Fe_{10.2}O_{19}$ single crystal: a) at 293°K; b) at 77°K.

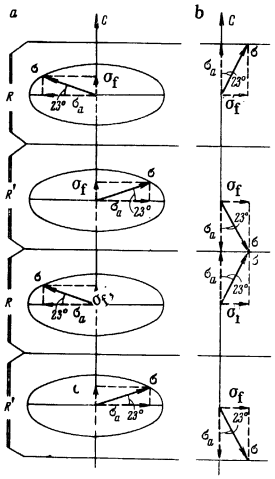

FIG. 3. Possible ordering schemes of the total magnetic moments (σ) of the R and R′ blocks in the unit cell of $BaSc_{1.8}Fe_{10.2}O_{19}$ at 293°K.

inclined at an angle of about 23° to the C axis, so that the axial components of the magnetic moment are in antiphase. The calculated experimental value of the reflection intensities for the model shown in Fig. 3b are listed in Table II. The convergence factor is ≈10%.

We must mention that the neutron-diffraction pattern shown in Fig. 2a includes weak reflections of purely nuclear origin at points forbidden by the space group ($P6_3/mmc$) of the crystal. The same reflections are present also in the pattern shown in Fig. 2b as well as, in a much weaker form, in the diffraction patterns for the compositions $BaSc_{1.2}Fe_{10.8}O_{19}$ and $BaSc_{1.4}Fe_{10.6}O_{19}$. These reflections are due to the presence of neutrons of $\lambda/2$ wavelength and to slight distortions of the symmetry of the crystal caused by the introduction of scandium ions which have a larger ionic radius than iron (0.83 Å for scandium and 0.67 Å for iron).

Cooling to 77°K altered considerably the neutron-diffraction pattern (Fig. 2b). In this case, the structure reflections (even values of l) had practically no magnetic contribution but fairly strong doublet superstructure reflections of magnetic origin were observed. The doublet peaks were found to be located symmetrically on both sides of the points corresponding to the $00l$ reflections, with odd values of l, which were forbidden by the space group of the crystal.

In our earlier papers,[13, 15] we considered the model

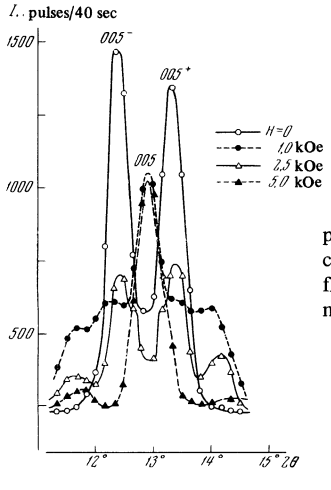

FIG. 4. Neutron-diffraction patterns of a $BaSc_{1.8}Fe_{10.2}O_{19}$ crystal in the region of the 005 reflection at 77°K, as a function of a magnetic field $H \perp c$.

of a polytypic helicoidal magnetic structure which was manifested by pairs of reflections located symmetrically with respect to the structure reflections. In the present case, we observed a similar pattern except that the symmetry centers of the superstructure pairs were at the positions of the forbidden reflections with $l = 2n + 1$. The forbiddenness of the reflections with odd values of l could be lifted if, for example, the projections of the total magnetic moment onto the basal plane in the R and R′ blocks were in antiphase, i.e., if they were turned through 180°. Since we observed doublets along the forbidden directions, the question arose whether the antiphase helicoidal structure existed in the investigated crystal. In the case of such a structure, the total magnetic moments of the R and R′ blocks would form two helically ordered sublattices with antiphase directions of rotation.

This model was supported by the results of our investigation of the behavior of the "satellites" when a magnetic field was applied perpendicular to the scattering vector ε. Figure 4 shows the behavior of the satellites (in the region of the reflection 005) for $BaSc_{1.8}Fe_{10.2}O_{19}$. When the magnetic field intensity was increased, the intensity of the $005^{\pm}$ magnetic doublet rapidly decreased and the doublet practically disappeared in H = 5 kOe. The distortion of the satellite reflection profiles was due to the appearance of helices with periods larger and smaller than that of the principal helix. Moreover, when the intensities of the main doublet peaks decreased with increasing magnetic field intensity, an antiphase 005 reflection was observed. Thus, when the helicoidal magnetic structure was destroyed, regions were formed in which the spin axes in the R and R′ blocks were exactly in antiphase. In still stronger fields, the antiphase orientation should be disturbed, but our magnetic investigations showed that the magnetization curve did not reach saturation in fields up to 15 kOe and it retained its constant slope, indicating that the antiphase orientation was conserved.

Figure 5 shows the dependences of the intensities of the 004 basal reflection and the 005 satellite reflection on the magnetic field intensity. Curve 5 in this figure shows that the helicoidal structure was destroyed completely in fields of 2.5–3.0 kOe. In these fields, the intensity of the basal reflection 004 (curve 2) began to increase but this increase was slower than that at 293°K because of the antiphase ordering in the crystal.

The period of the helicoidal structure of $BaSc_{1.8}Fe_{10.2}O_{19}$ was ≈141 Å along the C axis. The helicoidal period τ was a multiple of the unit cell parameter c. Each superperiod (141 Å) contained exactly six unit cells, i.e., twelve R-type blocks. This observa-

Table II. Calculated and experimental data for the model of a $BaSc_{1.8}Fe_{10.2}O_{19}$ single crystal in Fig. 3b

$00l$	F_n^2	F_m^2	I_{theor}	$I_{theor}^{E_p E_s}$	I_{exp}
002	6.81	8.58	78.33	49.50	48.70
004	10.69	204.78	95.00	63.95	60.00
006	5.38	82.81	29.55	25.00	25.00
008	116.21	215.21	402.91	91.20	78.19
0010	119.46	99.00	278.05	90.80	76.21

Here, F_n and F_m are, respectively, the nuclear and magnetic structure factors.

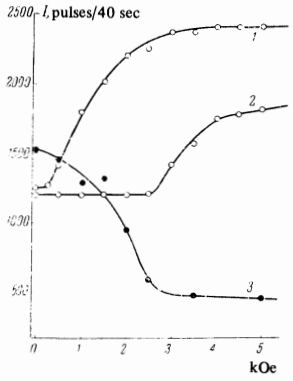

FIG. 5. Dependences of the reflection intensities on a magnetic field $H \perp c$ for $BaSc_{1.8}Fe_{10.2}O_{19}$: 1) 004 reflection, T = 293°K; 2) 004 reflection, T = 77°K; 3) 005^- reflection, T = 77°K.

tion, as well as similar observations for other $BaSc_xFe_{12-x}O_{19}$ compositions, confirmed the validity of our earlier conclusions on the block ordering of spins in hexagonal ferrite. Assuming an antiphase helicoidal orientation of the directions of the total magnetic moments of the neighboring R and R′ blocks in the $BaSc_{1.8}Fe_{10.2}O_{19}$ ferrite, we found that the phase angle of the projection in the basal plane was $\varphi = 150°$. The value of the phase angle φ for this variant of the helicoidal ordering was related to the period τ and the unit cell parameter c by the relationship $\varphi = \pi[1 - (c/\tau)]$.

A study of the nonbasal reflections showed that there was no appreciable magnetic contribution at 77°K. This confirmed the magnetic data on the presence of an easy magnetization axis, coinciding with the C axis. Calculations suggested a model in which the total magnetic moments of the blocks were generators of a cone whose axis coincided with the C axis (Fig. 6a). The projection of the total magnetic moment of the whole cell on the basal plane determined the structure factor of the helical reflection doublets which the axial component of the magnetic moment represented the magnetic contribution to the nonbasal reflections. The best convergence factor ($\approx 17\%$) for this model was obtained when the cone vertex half-angle was 30°.

Comparison of the calculated and experimental values of the basal reflection intensities is made in Table III. In estimating the convergence factor, we compared the total value of the intensities for the satellite pairs because of the anomalous behavior of I_{exp} of the $003^{\pm}$, $007^{\pm}$, and $0011^{\pm}$ doublets.

C. $BaSc_{1.2}Fe_{10.8}O_{19}$ ferrite. The basal reflection patterns, obtained at 293 and 77°K for this ferrite, are given in Fig. 7. The pattern at 293°K differed little from the pattern for $BaFe_{12}O_{19}$ and contained no magnetic contribution. However, the nonbasal reflections had a considerable magnetic contribution. On the basis of these observations, we assumed a uniaxial model, similar to that of $BaFe_{12}O_{19}$, in which the magnetic moments of the ions were aligned along the C axis or were slightly inclined to this axis. The diffraction pattern at 77°K (Fig. 7b) included superstructure doublets, which were similar to but much weaker than the doublets observed for $BaSc_{1.8}Fe_{10.2}O_{19}$. Therefore, the antiphase helicoidal magnetic ordering model assumed for the ferrite discussed here (Fig. 6b) was similar to that of $BaSc_{1.8}Fe_{10.2}O_{19}$ but had a smaller cone vertex half-angle of $\approx 12°$. An increase in the distance between the satellites indicated a new period of the helix, which was 70 Å, i.e., equal to three unit cells along the C axis. Thus, a complete revolution of the helix enclosed six R-type blocks. The phase angle for the helical component σ_h of the total magnetic moment σ, projected onto the basal plane, was 120°. The calculated and experimental data for a series of the basal reflections of the $BaSc_{1.2}Fe_{10.8}O_{19}$ ferrite are given in Table IV.

When a magnetic field was applied perpendicular to the scattering vector, the helical structure was destroyed and an antiphase peak appeared, as in the preceding case. However, in fields up to 5 kOe, the satellites were still fairly prominent, which indicated a more "rigid" structure of the helix in this case.

D. $BaSc_{1.4}Fe_{10.6}O_{19}$ ferrite. This composition was investigated in order to determine the nature of the transition of the antiphase helicoidal model of the $BaSc_{1.8}Fe_{10.2}O_{19}$ ferrite to the model of $BaSc_{1.2}Fe_{10.8}O_{19}$. It was found that the compound considered here had an intermediate structure with a period $\tau \approx 91$ Å, which represented approximately 3.9 unit cells along the C axis. The phase angle was $\varphi \approx 135°$ and the cone vertex half-angle was ~20°. The anomalies reported for the other compositions were observed also for the ferrite

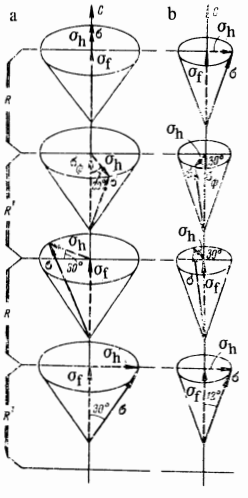

FIG. 6. Possible ordering schemes of the total magnetic moments of the R and R′ blocks in the unit cells of a) $BaSc_{1.8}Fe_{10.2}O_{19}$ and b) $BaSc_{1.2}Fe_{10.8}O_{19}$ at 77°K.

Table III. Calculated and experimental data for a $BaSc_{1.8}Fe_{10.2}O_{19}$ single crystal at 77°K

00l	F^2	I_{theor}	$I_{theor} E_p E_s$	I_{exp}
002	6,81	75,70	49,91	52,40
003^-	39,94	34,90	28,78	22,56
003			54,78	54,14
003^+	39,56	30,72	26,00	31,58
004	10,69	62,89	47,23	51,28
005^-	256,96	133,58	72,37	87,61
005			143,11	157,17
005^+	256,00	125,11	70,74	69,56
006	5,38	20,71	18,80	18,80
007^-	4,67	1,66	1,66	2,00
007			3,26	5,00
007^+	4,62	1,60	1,60	3,00
008	116,2	385,48	100,08	66,94
009^-	178,4	51,91	40,70	32,26
009			79,60	62,36
009^+	173,19	48,37	38,90	30,10
0010	119,46	271,61	94,26	70,34
0011^-	21,90	5,26	5,20	5,00
0011			9,90	11,10
0011^+	20,43	4,79	4,70	6,10

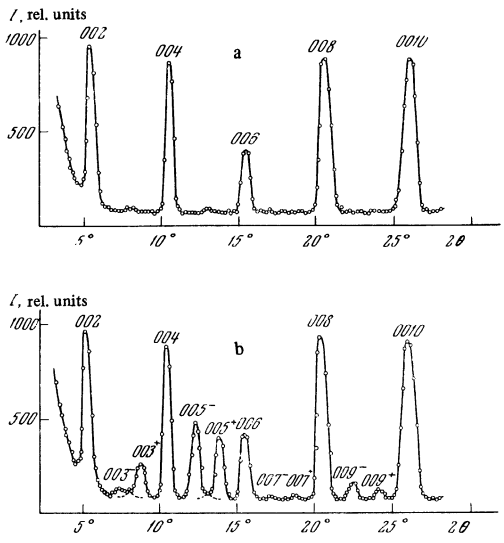

FIG. 7. Neutron-diffraction patterns of a family of the basal planes of a $BaSc_{1.2}Fe_{10.8}O_{19}$ single crystal: a) at 293°K; b) at 77°K.

discussed here but they were weaker.

E. $BaSc_{0.5}Fe_{11.5}O_{19}$ ferrite. The neutron-diffraction patterns of this ferrite were practically identical with the patterns of pure $BaFe_{12}O_{19}$. This indicated that the concentration of scandium (one ion per unit cell) was insufficient to disturb the axial collinear structure.

3. DISTRIBUTION OF Sc^{3+} IONS IN THE $BaSc_xFe_{12-x}O_{19}$(M) SYSTEM

Unfortunately, the similar values of the nuclear scattering amplitudes of iron and scandium ($+0.96 \times 10^{-12}$ and $+1.18 \times 10^{-12}$ cm, respectively) prevented us from determining with certainty the positions of ions from the intensities of the nuclear components of the diffraction patterns. However, the replacement of iron by scandium had a stronger effect on the magnetic contribution to the diffraction pattern. An investigation of the values of the magnetic contributions to the reflections indicated that the most likely positions of scandium were the 4f octahedral positions and the 2b fivefold positions, with z = 0.1889 and z = 0.25, respectively. When the concentration of scandium was increased, Sc^{3+} ions occupied first the 4f positions and then the fivefold sites.

4. DISCUSSION OF RESULTS

The magnetic structures described in the present paper extend the range of new spin configuration which have been reported first in [15]. Such spin ordering, combining the elements of the collinear and noncollinear spin moment configurations, is evidently very typical of hexagonal ferrites. This class of ferrites has a very large c/a ratio and a wide range of crystallographically different vacancies in the oxygen packing. Consequently, when various cations, which are attracted to definite vacancies in the crystal structure, are introduced into these ferrites, we may have a case in which some cations occupy only octahedra of one type. If these cations are not magnetically active, the exchange coupling between groups of spins in the unit cell may be disturbed locally. This gives rise to blocks whose moments may behave as if these blocks were independent structural units. Within such blocks the spin ordering is collinear. However, the directions of the spin axes may vary from block to block, forming angular, helical, antiphase, and other magnetic configurations.

Table IV. Calculated and experimental data for a $BaSc_{1.2}Fe_{10.8}O_{19}$ single crystal at 77°K

00l	F^2	I_{theor}	$I_{theor} E_p E_s$	I_{exp}
002	9,16	103,33	45,94	34,25
003⁻	40,03	3,92	3,90	1,87
003			6,81	7,59
003⁺	38,60	2,93	2,91	5,62
004	14,32	80,94	43,71	33,37
005⁻	262,70	14,52	13,10	12,75
005			24,10	23,75
005⁺	251,40	12,12	11,00	11,00
006	3,47	13,31	12,00	12,50
007⁻	4,72	1,93	1,93	1,50
007			3,75	3,37
007⁺	4,48	1,82	1,82	1,87
008	128,50	357,22	39,00	44,50
009⁻	181,00	5,50	5,20	3,75
009			9,80	5,87
009⁺	170,80	4,80	4,60	2,12
0010	110,05	250,09	47,30	46,75

The intensity of the superstructure reflections is governed by the value of the helical component of the magnetic moment, the wave vector of the structure, and the localization of the corresponding spin density, we may attribute the observed effects to a considerable asphericity of the spin density of the Fe^{3+} ions in the crystal lattice.

The neutron-diffraction results obtained make it possible to provide an alternative explanation of the considerable reduction of the saturation moment of scandium-substituted ferrites at low temperatures.[12] The results of the present investigation indicate that this decrease is the result of a rearrangement of the spin configuration.

The authors are grateful to T. M. Perekalina and V. P. Cheparin for the supply of samples and the magnetic data, as well as for their constant interest in this investigation.

[1] V.Adelkcöld, Ark. Kemi Mineral. Geol. 12A, No. 29, 1–9 (1938).
[2] P. B. Braun, Philips Res. Rep. 12, 491 (1957).
[3] J. J. Went, G. W. Rathenau, E. W. Gorter, and G.W. van Oosterhout, Philips Tech. Rev. 13, 194 (Jan. 1952).
[4] L. G. van Uitert, J. Appl. Phys. 28, 317 (1957).
[5] E. W. Gorter, Proc. Inst. Elec. Engrs. (London), 104B, Suppl. 4, 255, 265 (1957).
[6] P. W. Anderson, Phys. Rev. 79, 705 (1950).
[7] H. A. Kramers, Physica 1, 182 (1934).
[8] E. F. Bertaut, A. Deschamps, P. Pauthenet, and S. Pickart, J. Phys. Radium 20, 404 (1959).
[9] F. K. Lotgering, U. Enz, and J. Smit, Philips Res. Rep. 16, 441 (1961).
[10] H. B. G. Casimir, J. Smit, U. Enz, J. F. Fast, H. P. J. Wijn, E. W. Gorter, A. J. W. Duyvesteyn, J. D. Fast, and J. J. de Jong, J. Phys. Radium 20, 360 (1959).
[11] A. Tauber, J. A. Kohn, and R. O. Savage, J. Appl. Phys. 34, 1265 (1963).
[12] T. M. Perekalina and V. P. Cheparin, Fiz. Tverd.

Tela **9**, 3205 (1967) [Sov. Phys.-Solid State **9**, 2524 (1968)].
[13] V. A. Sizov, R. A. Sizov, and I. I. Yamzin, Zh. Eksp. Teor. Fiz. **53**, 1256 (1967) [Sov. Phys.-JETP **26**, 736 (1968)].
[14] R. Nathans, S. J. Pickart, and H. A. Alperin, J. Phys Phys. Soc. Japan **17**, Suppl. B-3, 7 (1962).
[15] T. M. Perekalina, V. A. Sizov, R. A. Sizov, I. I. Yamzin, and R. A. Voskanyan, Zh. Eksp. Teor. Fiz. **52**, 409 (1967) [Sov. Phys.-JETP **25**, 266 (1967)].

Translated by A. Tybulewicz
96